Electron structure of single and interacting hydrogen impurities in free-electron-like metals

J. K. Nørskov
Institute of Physics, University of Aarhus, 8000 Aarhus C, Denmark
(Received 10 October 1978)

Recent progress in the theoretical description of hydrogen impurities in metals, as described by the jellium model, and their interaction mutually and with vacancies are described. In addition to giving a detailed account of the author's contribution, the paper presents new results for the spectra of the hydrogen-induced states. These show for single interstitial hydrogen a doubly occupied bound state, while substitutional hydrogen has an atomic resonance in the conduction band. In both cases the state is situated just below the "local bottom of the band," as defined by the clean-metal effective potential at the impurity site. When two such states interact, both the bonding and the antibonding molecular orbitals get filled except at the lowest metallic densities, and a repulsive hydrogen-hydrogen interaction results. Spin-polarized Δ self-consistent-field calculations of the impurity excitation energies are presented. The results compare well with the one-electron binding energies of the bound states and with the excitation energies calculated by Vinter. The hydrogen impurity spectra presented can therefore be expected to represent approximately experimental excitation spectra of interstitial and substitutional hydrogen in free-electron-like metals.

I. INTRODUCTION

Hydrogen impurities in metals have been the subject of a large number of experiments, including studies of heats of solution,[1] diffusion properties,[2] and interactions with defects.[3] Progress in the theoretical description of the electron structure of hydrogen in metals has been slower. This is because a complete theory must take into account both the local nature of the strong interactions with nearest neighbors as well as the extended nature of all electron states within the metal conduction band and do this in a self-consistent way. The model calculations made so far have typically emphasized one of these aspects at a time.

Recently, cluster calculations started to appear in which only the hydrogen impurity and the nearest neighbors are included in a molecular self-consistent-$X\alpha$-multiple-scattering (SCF-$X\alpha$-MS) calculation.[4] This approach emphasizes the local effects, and the hope is that convergent results will appear as the cluster size is increased. The drawback of a method like this is that the screening by the conduction electrons is not described properly. On the other hand, the effects of, e.g., the more localized d electrons in transition metals should be incorporated reasonably in this way.

Most efforts so far have been put into the other extreme, the *jellium model*, in which the ion cores of the metal are smeared out to an infinite positive background. In this model, primarily the (screening) effects of the free-electron-like conduction electrons are accounted for, so it is most appropriate for describing such simple metals as Na, Mg, and Al. Model calculations of this kind do have qualitative bearings for transition metals too, however, in establishing the effect of the sp conduction electrons on the impurity.

It should be stressed that the true impurity problem involves other effects, e.g., interactions with core and d electrons and effects due to lattice relaxation. In the free-electron-like metals, where the ion-core contribution to the total potential is small relative to the impurity-induced potential, the electron structure can be expected to be relatively well described in this model. The total energy, on the other hand, is a delicate balance between many competing effects, and, e.g., in the free-electron-like metals the ion-core contribution should be taken into account. Attempts have been made to include the ionic pseudopotential lattice in a perturbative way.[6,18] For the coherence of the presentation, however, the present paper deals only with the pure-jellium results.

The first, self-consistent calculations of the nonlinear screening of a proton, which include exchange and correlation through the local-density approximation,[5] have been made by Popovic and Stott[6] and Almbadh *et al.*[7] Since then a number of groups have published similar results.[8-11] Extensions to systems where the hydrogen is trapped in a vacancy have also been made.[10,11] Such other impurities as He,[10-12] Li,[10,13] and F and Ne,[14] have also been treated within the jellium model.

In the Sec. II the main results of the hydrogen calculations will be briefly reviewed. They have primarily been concerned with the induced electron density (screening charge) and interaction energy at different jellium densities. In the present work this is completed with a presentation of the impurity-induced density of states $\Delta D(\epsilon)$, which provides a basis for an understanding of the

impurity-induced electron structure. The characteristics of $\Delta D(\epsilon)$ for an isolated as well as a vacancy-trapped hydrogen impurity are shown and used as a starting-point for a discussion of the extent to which the impurity-induced electron structure depends on the local environment. The relation of ΔD to the true excitation spectrum is also discussed. Spin polarized ΔSCF (change in self-consistent total-energy) calculations of the excitation energy of the bound impurity electrons are presented and compared with the excitation energy extracted from ΔD and from more advanced calculations, including a nonlocal energy-dependent self-energy (Sec. IV).

In Sec. V the preliminary results of Ref. 15 for the effect of the conduction electrons on the interaction between two hydrogen impurities are completed and discussed on the basis of the changes in the induced density of states as two hydrogen impurities approach each other.

First, however, in Sec. III a brief summary is given of the density-functional formalism, including the local density approximation. The present method for the numerical handling of the problem is also described. For a full presentation of this, the reader is referred to the original papers by Gunnarsson and Hjelmberg[16] and Hjelmberg.[17]

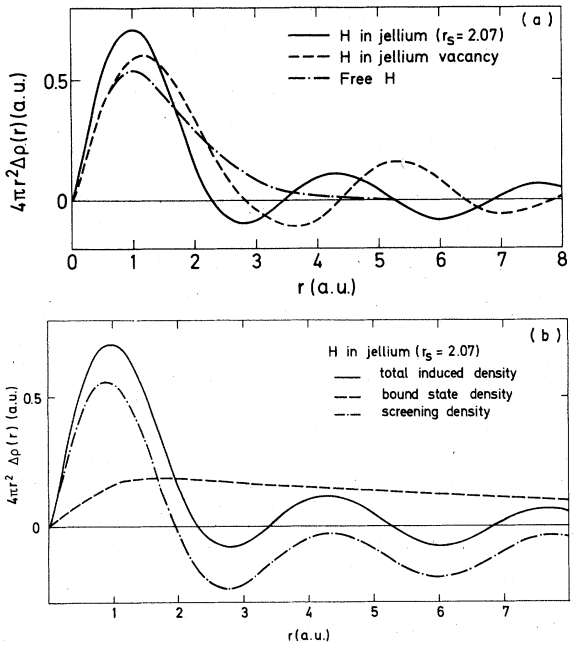

FIG. 1. Induced density $4\pi r^2\Delta\rho(r)$ for hydrogen in jellium for $r_s = 2.07$ corresponding to Al: (a) compared with that of free hydrogen and hydrogen in a jellium vacancy; (b) decomposed into bound-state and screening-charge contributions.

II. JELLIUM-MODEL RESULTS FOR INDUCED DENSITY AND ENERGY

For convenience, a few central results of the jellium model for the hydrogen impurity problem are summed up in this section. The impurity-induced electron density is a central quantity in the description of the impurity-induced electron structure. In the jellium model it is spherically symmetrical, fully described by its radial part $4\pi r^2\Delta\rho(r)$. In Fig. 1(a) the characteristic behavior of this quantity is shown for jellium parameters corresponding to Al ($r_s = 2.07$). The density parameter r_s is defined by the average conduction-electron density ρ_0: $\rho_0^{-1} = \frac{4}{3}\pi r_s^3$. In the figure, the induced density is compared with that of a free hydrogen atom. It is seen that, apart from the Friedel oscillations for large r, the induced density also departs from that of free hydrogen in the region close to the proton, where a further buildup of charge takes place. This is observed quite generally, and the enhancement increases with decreasing r_s (increasing ρ_0).[7-11] This trend is found again when the proton is moved from the bulk of the metal to a vacancy. In jellium, a vacancy is modeled by taking out a Wigner-Seitz cell of the positive background. As shown in Fig. 1(a), the buildup decreases in accordance with the fact that the conduction electron density is lower here.[10,11]

Owing to the pileup of charge, the proton is screened out very efficiently. The screening length is as small as 0.6 a.u. and almost independent of r_s.[7] This is in contrast to the linear screening length and shows that a nonlinear calculation is necessary for the strong proton potential.[7]

Although such experimental energies as the heat of solution can be accounted for properly only by having the interaction with the ionic cores and possible relaxation effects included, the part due to the impurity–conduction-electron interactions has a certain interest, particularly its dependence on r_s. In Table I, therefore, the jellium energies E_H defined as the energy of hydrogen in jellium minus the energy of the pure-jellium substrate are collected.

In addition to the general agreement between the results of several different groups, Table I shows the general feature that E_H increases with decreasing r_s for r_s in the metallic range. In Ref. 11 this increase was correlated with the increase in charge pileup or contraction. It is therefore not surprising that the decrease in charge buildup observed, when moving the hydrogen impurity from the bulk into an existing vacancy (see Fig. 1), is accompanied by a decrease in energy. Actually, the interaction with the conduction electrons alone gives a substantial attraction of the hydrogen atom

TABLE I. Comparison of energies for hydrogen in jellium at different r_s by different authors. The energies should be compared with the local spin-density value of 13.39 eV for the free hydrogen atom.

	E_H (eV)			
r_s	Almbladh *et al.*	Manninen *et al.*	Zaremba *et al.*	Present work
2.07 (Al)	−12.3	−12.7	−12.3	−12.1
2.65 (Mg)	−14.2	−14.3	−14.1	−14.4
3.93 (Na)	−15.0		−15.0	−15.0

to the vacancy, except for those metals with very low conduction-electron density (Na, Cs, etc.).[11]

Finally, all existing calculations show that a shallow doubly-occupied bound state exists for r_s in the metallic region.[7-11] This implies that hydrogen in metals should be regarded as a screened H^- ion. However, the possibility of the existence of a spin-unrestricted solution with only one bound electron has not been examined. We will return to this question in Sec. IV.

III. THEORETICAL METHOD

A. Kohn-Sham scheme

In solving the complicated many-body problem of an impurity in a metal, the density-functional formalism of Hohenberg, Kohn, and Sham[5,19] is used. Here the N electron problem is converted into N Schrödinger-like one-electron equations, which must be solved self-consistently [I omit spin indices for simplicity; atomic units (Ry) are used unless otherwise stated]:

$$-\nabla^2\phi_i(\vec{r}) + V_{eff}(\vec{r})\phi_i(\vec{r}) = \epsilon_i\phi_i(\vec{r}),$$

$$\rho(\vec{r}) = \sum_i^{occ} |\phi_i(\vec{r})|^2, \tag{1}$$

$$V_{eff}(\vec{r}) = V_{ext}(\vec{r}) + \int \frac{2\rho(\vec{r})}{|\vec{r}-\vec{r}'|} d\vec{r}' + V_{xc}(\vec{r}).$$

The effective one-electron potential V_{eff} consists of the external potential V_{ext}, the average electrostatic potential, and a potential $V_{xc}(\vec{r})$, which describes the exchange and correlation effects. For V_{xc} the local- (spin-) density approximation is used.[20] This is justified by the success of this approximation in describing systems as different as atoms and molecules and clean metals,[20] which exhibit the localized as well as the extended properties of the impurity-in-metal problem. In this approximation the ground-state energy is given from $\rho(\vec{r})$ by[5]

$$E = \sum_i^{occ} \epsilon_i - \int V_{eff}(\vec{r})\rho(\vec{r})d\vec{r} + \int V_{ext}(\vec{r})\rho(\vec{r})d\vec{r} + \int\int \frac{\rho(\vec{r})\rho(\vec{r}')}{|\vec{r}-\vec{r}'|} d\vec{r}\,d\vec{r}' + \int \epsilon_{xc}(\rho(\vec{r}))\rho(\vec{r})d\vec{r}. \tag{2}$$

Both V_{xc} and the exchange-and-correlation energy density ϵ_{xc} have been taken from Ref. 20.

B. Green's-function method

In the present problem the quantities of interest are the impurity-induced density $\Delta\rho(\vec{r}) = \rho(\vec{r}) - \rho^0(\vec{r})$, density of states $\Delta D(\epsilon) = D(\epsilon) - D^0(\epsilon)$, and energy $\Delta E = E - E^0$ (a superscript 0 is used to denote a pure-metal value). Instead of solving Eq. (1) directly for the ϕ_i's, we solve the equivalent Dyson equation for the Green's function G:

$$G(\vec{r},\vec{r}',\epsilon) = G^0(\vec{r},\vec{r}',\epsilon) + \int\int G^0(\vec{r},\vec{r}'',\epsilon) \times \Delta V_{eff}(\vec{r}'') \times G(\vec{r}'',\vec{r}',\epsilon)\, d\vec{r}''. \tag{3}$$

Equation (3) involves the impurity-induced effective potential $\Delta V_{eff} = V_{eff} - V_{eff}^0$. From $\Delta G = G - G^0$, $\Delta\rho$ and ΔD can be found directly:

$$\Delta\rho(\vec{r}) = -\frac{1}{\pi}\int_{-\infty}^{\epsilon_F} d\epsilon\, \mathrm{Im}\,\Delta G(\vec{r},\vec{r},\epsilon) \tag{4}$$

and

$$\Delta D(\epsilon) = -\frac{1}{\pi}\int d\vec{r}\, \mathrm{Im}\,\Delta G(\vec{r},\vec{r},\epsilon). \tag{5}$$

From $\Delta\rho(\vec{r})$, ΔE can be found through Eq. (2).

Now the method exploits the fact, that owing to the screening by the conduction electrons, $\Delta\rho$ and ΔV_{eff} are almost totally localized within a region (here chosen as a sphere of radius R) centered at the impurity. This has two implications: First, if we choose a finite basis set $\{\varphi_n\}_N$ which is approximately complete in the region of interest, we need only the projection of ΔG onto $\{\varphi_n\}_N$ to get the induced density $\Delta\rho(\vec{r})$:

$$\Delta\rho(\vec{r}) = -\frac{1}{\pi}\int_{-\infty}^{\epsilon_F} P\,\mathrm{Im}\,\Delta G(\vec{r},\vec{r}',\epsilon)P\Big|_{\vec{r}'=\vec{r}} d\epsilon = -\frac{1}{\pi}\sum_{nn'}^{N}\int_{-\infty}^{\epsilon_F} \langle\varphi_n|\,\mathrm{Im}\,\Delta G\,|\varphi_{n'}\rangle d\epsilon \times \varphi_{n'}(\vec{r})\varphi_n(\vec{r}). \tag{6}$$

where P is the projection operator $P(\vec{r},\vec{r}') = \sum_n \varphi_n(\vec{r})\varphi_n(\vec{r}')$. Second, the Dyson integral equation (3) reduces to

$$PGP = PG^0P + PG^0P\Delta V_{eff}PGP \tag{7}$$

because terms like $PG^0P\Delta V_{eff}(1-P)GP$, $PG^0(1-P)\Delta V_{eff}PGP$, and $PG^0(1-P)\Delta V_{eff}(1-P)GP$ are small and might be neglected.[13,14]

Equation (7) can be expressed as a matrix equation of dimension N

$$\underline{G}_A = \underline{G}^0_A + \underline{G}^0_A\,\underline{\Delta V}_{eff,A}\underline{G}_A\,, \tag{8}$$

where A denotes the matrix elements between the local basis functions φ_n. Like Eq. (1), this equation must be solved self-consistently. In each iteration $\Delta\rho(\vec{r})$ and thereby ΔV_{eff} can be found through Eq. (6). When convergence is reached, ΔE is obtained from Eqs. (6) and (2).

Because of the infinite extension of the wave functions in the metallic system, ΔG itself is not as localized as $\Delta\rho$. This means that $\Delta D(\epsilon)$ cannot be obtained directly from $\Delta\underline{G}_A$, but $\Delta\underline{G}_A$ will give the local induced density of states

$$\Delta D^{\mathrm{L}}(\epsilon) = -\frac{1}{\pi}\,\mathrm{Tr}(\mathrm{Im}\Delta\underline{G}_A)\,.$$

This quantity projects out the part of the density of states with weight within the sphere of radius R. It is particularly useful if further projections are needed as, e.g., for H_2, where the antibonding (Σ_u) states near the molecule are of great interest. However, ΔD^{L} does depend on R, though the important structure is included in ΔD^{L}, as will be discussed later. In the spherically symmetric cases the contribution $\Delta D^{\mathrm{NL}}(\epsilon)$ to $\Delta D(\epsilon)$ from outside the perturbed sphere can be found and added. This is because the asymptotic behavior of $-1/\pi\,\mathrm{Im}\Delta G(\vec{r},\vec{r},\epsilon)$ is known in this case. For $\sqrt{\epsilon}r$ ($r = |\vec{r}|$) large[21]

$$-\frac{1}{\pi}\,\mathrm{Im}\Delta G_l(r,r,\epsilon) \simeq c_l(\epsilon)\,\frac{\sin[2\sqrt{\epsilon}r + \eta_l(\epsilon)]}{r^2}\,. \tag{9}$$

Such a relation exists for any angular momentum value l. An expression like this can be fitted to the calculated values just inside the sphere radius R, and $c_l(\epsilon)$ and $\eta_l(\epsilon)$ can be determined. Then ΔD^{NL} can be found as

$$\begin{aligned}\Delta D^{\mathrm{NL}}(\epsilon) &= \int_R^\infty -\frac{1}{\pi}\,\mathrm{Im}\Delta G(r,r,\epsilon)4\pi r^2\,dr \\ &= \sum_l 2\pi[c_l(\epsilon)/\sqrt{\epsilon}]\cos[2\sqrt{\epsilon}R + \eta_l(\epsilon)]\,.\end{aligned} \tag{10}$$

C. Basis functions

The virtue of the present method is that it is in principle quite general. No assumptions about, e.g., spherical symmetry have been made. It is therefore possible to handle an impurity like H_2. Neither has anything been assumed about the metallic host, the effects of which are included through G^0. In the present work the jellium model has been used and G^0 is simply the free-electron Green's function. For impurities in a jellium vacancy the free-electron G^0 is still used and a calculation is made for a vacancy with and without the impurity to get the impurity-induced quantities. However, other models of the substrate are possible, as, e.g., in the chemisorption calculations,[16,17] where a semi-infinite jellium model is used.

The price paid for the generality and calculational simplicity of the method is that we have had to make the two approximations behind Eq. (7). Since they both hinge upon the completeness of the finite basis set, the validity of Eq. (7) can always be improved by increasing N, the number of basis functions. The applicability of the method therefore depends on whether a basis set can be found small enough to make the problem tractable.

It has appeared that 8–10 radial functions of the type

$$R_n(r) = \sum_{\nu=0}^{N-1} c^{\alpha}_{n\nu} r^{\nu} e^{-\alpha r} + \sum_{\nu=0}^{N-1} c^{\beta}_{n\nu} r^{\nu} e^{-\beta r}$$

in connection with spherical harmonics with l values up to 2 are sufficient to get convergence both in the atomic as well as the molecular im-

TABLE II. Basis-set parameters and total-energy correction (see text) in absolute numbers and relative to the calculated total energy. The correction for H_2 is shown for a range of H-H distances (R_0).

Impurity	Basis set				Correction	
	N	R (a.u.)	α (a.u.)	β (a.u.)	(eV)	(%)
H	9	8	1	0.5	0.15	1.1
H_2 (R_0=1.0 a.u.)	8	7	1.69	1.0	0.15	0.5
H_2 (R_0=1.2 a.u.)					0.21	0.7
H_2 (R_0=1.4 a.u.)					0.40	1.3
H_2 (R_0=1.7 a.u.)					0.58	1.9
H_2 (R_0=2.0 a.u.)					0.72	2.3

purity cases. In the latter case the basis functions are centered at the molecular midpoint. To avoid systematic errors due to the finiteness of the basis set, the calculated ΔE for the impurity in jellium has been corrected by the difference found between the results of the present method for an isolated H atom and H_2 molecule, and those of accurate atomic and molecular local density approximation calculations for these simple systems.[20]

In Table II the corrections are shown for the two basis sets used in the calculations. In both cases the corrections are seen to be relatively small. The error in the H_2 calculations increases with R_0, the internuclear distance, indicating that the one-center expansion becomes worse the further away from the center the density and potential peaks. This means that the results for large R_0 must be interpreted with some care.

In both cases reasonable changes in the basis-set parameters (shown in Table II) induce only small changes in the total energies. For a further discussion of the validity of the method, the reader is referred to Ref. 17. Here I will only point out the good agreement with the results of the other methods mentioned in connection with Table I.

IV. SINGLE IMPURITY

A. Induced density of states

In this section the earlier published results for the induced density and the energy of hydrogen in metals presented in Sec. II are supplemented with data for the induced density of states.

Figure 2 shows the induced density of states for H in Al-jellium ($r_s = 2.07$). Both the total (ΔD^L) and the s ($l = 0$) part (ΔD_s^L) of the local induced density of states are shown. It is seen that almost all the structure is due to the s part ΔD_s^L. Furthermore, ΔD_s^L is compared with ΔD_s, where the nonlocal correction of Eq. (10) has been added. It is seen that the prime effect of including ΔD_s^{NL} is that the oscillatory behavior is reduced and only the antiresonance in the bottom of the band survives as a $1/\sqrt{\epsilon}$ divergence as $\epsilon \to 0$. Therefore, the information contained in ΔD_s^L and ΔD^L is the same: The extra electron connected with the shallow bound state is screened out primarily by the conduction electrons with the lowest energy, i.e., in the bottom of the band. Because these electrons have a long wavelength, the screening cloud is very extended [see Fig. 1(b)], the extremely extended bound electrons are screened out completely, and only the localized, hydrogenlike induced density survives, as shown in Fig. 1(b). This behavior of ΔD^L, ΔD_s^L, and ΔD_s is typical for hydrogen in jellium at metallic densities.

Also the position ϵ_b of the bound state relative to the bottom of the band varies little on an absolute

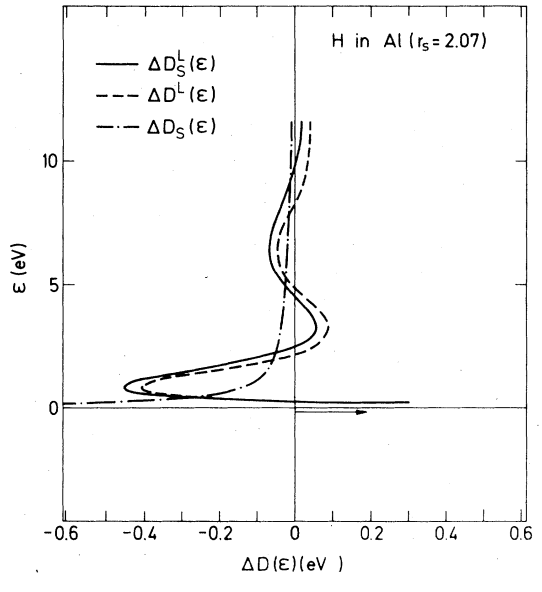

FIG. 2. Local (ΔD^L), s part of the local (ΔD_s^L) induced density of states, and s-part (ΔD_s) of the total induced density of states for hydrogen in jellium for $r_s = 2.07$ corresponding to Al.

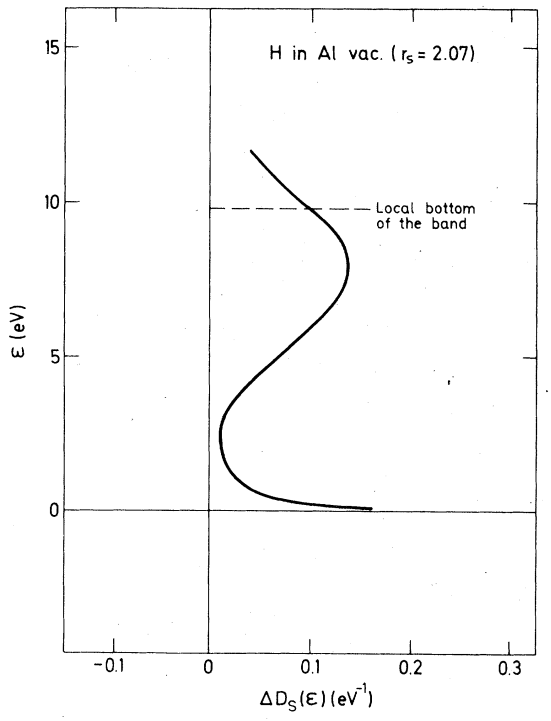

FIG. 3. The s-part of the induced density of states for hydrogen in jellium vacancy for $r_s = 2.07$ corresponding to Al.

scale. The general trend is that ϵ_b increases with increasing r_s.[22] Hydrogen impurities in jellium must therefore be regarded as heavily screened H^- ions. The reason why ϵ_b does not vary much on an absolute scale relative to that of free H^- is that when ϵ_b is small, even a small change in ϵ_b will alter the asymptotic behavior of the bound-state electron density, which behaves like $e^{-|\epsilon_b|^{1/2}r}$, substantially. Therefore even a very effective screening will only change ϵ_b a little.

B. Divergence for $\epsilon \to 0$

While the large positive values of $\Delta D_s^L(\epsilon)$ seen for small ϵ are due only to the shallowness of the bound state, the divergence noted for $\epsilon \to 0$ is always seen in $\Delta D_s(\epsilon)$. This effect, which was also noted by Inglesfield and Pendry[23] for He impurities, is due to the fact that for any potential of finite extent, the zero-order phase shift $\eta_s(\epsilon)$ behaves like $a\sqrt{\epsilon} + n\pi$ for $\epsilon \to 0$, where n is the number of bound states and a is a positive or negative constant, depending on whether or not n is zero.[24] Since the phase shift is related to the induced density of states through[25]

$$\Delta D_s(\epsilon) = \frac{2}{\pi}\frac{\partial \eta_s(\epsilon)}{\partial \epsilon},$$

this gives

$$\Delta D_s(\epsilon) \to (a/\pi)\epsilon^{-1/2} \quad \text{for } \epsilon \to 0.$$

In accordance with the above, a is seen to be negative in Fig. 2, where a bound state exists.

C. Hydrogen in vacancy

The opposite situation is illustrated in Fig. 3, where ΔD_s is shown for hydrogen in an Al ($r_s = 2.07$) vacancy. Here the $\epsilon \to 0$ divergence is positive, due to the fact that no bound state exists in this system. Instead, an almost completely filled, rather broad resonance is observed in the conduction band.

It is interesting to note that the resonance is positioned just below the effective potential V_{eff}^0 in the middle of the clean vacancy (see Fig. 3). The same effect is seen for other r_s values. This means that apart from the above-mentioned tendency of ϵ_b to follow the bottom of the band when r_s is varied, it also follows the "local bottom of the band" when going from bulk jellium to a vacancy. This is also seen when a hydrogen impurity is moved out through the surface.[26] It suggests that even in these cases the hydrogen should be regarded as essentially a screened H^- ion with an energy level displaced by approximately the free-atom affinity from the local bottom of the band. The level is then broadened when it lies within the conduction band. A similar picture holds for other adsorbate affinity levels.[27] A further example is the H_2 antibonding resonance discussed in Sec. V.

The correlation between conduction electron density, the charge pileup and the energy of an impurity when going from bulk jellium to a jellium vacancy, as mentioned in Sec. IIB, is another example of the importance of the local environment.

The local dependence of the electron structure on the environment must be related to the very small screening length λ found in the nonlinear calculations (cf. Sec. II). Because λ is small compared with, e.g., the radius of a vacancy, the impurity feels only the host-electron density $\rho^0(0)$ and effective potential $V_{\text{eff}}^0(0)$ in the middle of the vacancy, while it cannot see the rest of the host. $V_{\text{eff}}^0(0)$ then serves as the local energy zero and ϵ_b is determined relative to $V_{\text{eff}}^0(0)$ by $\rho^0(0)$. As discussed in Sec. IIIA, the absolute position of ϵ_b relative to $V_{\text{eff}}^0(0)$ is not very sensitive to changes in $\rho^0(0)$ due to the large extension of the state.

One might have expected at least the position of the very extended H^--like state to depend on a larger part of the environment. This is not so, though, because ΔD is totally determined by ΔV_{eff} and thereby by $\Delta\rho$ [see Eqs. (3) and (5)], which is much more localized. This also means that in a more realistic model for the metal, one where the ion-core contributions are taken into account, these only influence ΔD and thereby ϵ_b to the extent that $\Delta\rho$ is affected. For free-electron-like metals this effect is expected to be small, as noted in Sec. I.

D. Connection with excitation spectrum

The induced density of states of the Kohn-Sham scheme has no direct physical meaning. It should primarily be regarded as an aid in understanding the electronic structure, as illustrated in this and the next section. It is, however, tempting to interpret the induced density of states as an impurity excitation spectrum. Vinter[28] investigated this question for hydrogen and helium in jellium. Using

TABLE III. Excitation energies of the hydrogen-induced bound state in jellium at different r_s. One-electron and ΔSCF results of the present work are compared with the excitation energies calculated by Vinter (Ref. 28). (See text.)

r_s	$\lvert\epsilon_b\rvert + \epsilon_F$ (eV) Present work	Vinter	ΔSCF
2.07 (Al)	11.7	11.6	9.0
2.65 (Mg)	7.2		7.3
3.93 (Na)	3.6	3.5	3.8

the ground-state induced densities of the present work, he calculated the excitation spectrum from a nonlocal, energy-dependent self-energy. The resulting spectra for hydrogen are very close to the induced-state densities of the present work, as illustrated in Table III, where the binding energies (relative to the Fermi level) of the hydrogen-induced bound state are compared. The success of the one-electron theory must be attributed to the large extent of the bound-state density (small relaxation of final state), since no such agreement was seen for the tighter bound helium states.[28] In order to assure that the H^--like *spin-compensated* solution is really the ground state, *spin-unrestricted* calculations have been performed with only one bound electron. This H-like solution was, however, always found to have a higher total energy than the one with two bound electrons. The total-energy differences of these two self-consistent solutions are included in Table III (ΔSCF). This difference also measures the energy needed to promote one of the bound electrons to the Fermi level, and again good agreement with the one-electron result is found except, perhaps, at the highest density, though the trend is reproduced.

On this basis the induced density of states curves of Figs. 2 and 3 can be regarded with some confidence as typical excitation spectra of interstitial and substitutional hydrogen in jellium, and according to the arguments in Sec. IV C thus in free-electron-like metals. Furthermore, we can expect to be able to estimate the absolute position of the hydrogen-induced peak in the spectrum from our knowledge of the "local bottom of the band" at the impurity site.

V. H_2 IN JELLIUM

A. Binding energy

The interaction between two hydrogen impurities in a free-electron-like metal can also be studied in the jellium model. This is done by embedding an H_2 molecule in jellium and then study the binding energy $E_B(R_0)$ and spectrum as a function of the H_2 bond length R_0. Here $E_B(R_0)$ is defined as twice the energy of H in jellium minus the energy of H_2 in jellium. In Fig. 4, $E_B(R_0)$ is shown for H_2 in vacuum and in low-(Na) and high- (Al) density metals.[29] Already in low-density jellium the binding energy is substantially reduced and the equilibrium distance is increased. The curvature and thereby the H-H vibrational frequency are also reduced. At higher density the interaction is totally repulsive. We therefore expect the hydrogen-hydrogen interactions to be repulsive in most metals.

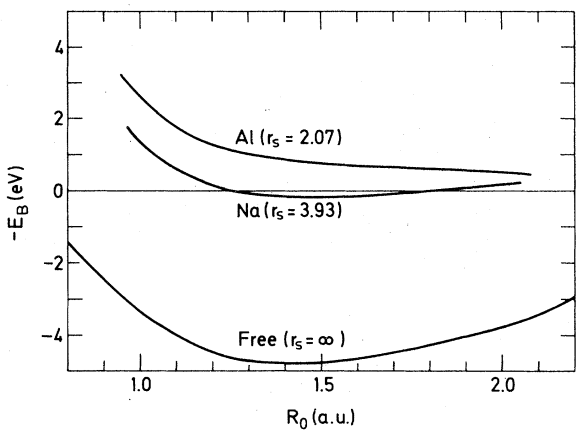

FIG. 4. Binding-energy curves for free hydrogen and hydrogen in jellium for $r_s = 2.07$ and 3.93, corresponding to Al and Na, respectively.

At $r_s = 3.93$ there is a tendency towards a dissociation barrier. This is also seen at other r_s values. Due to the smallness of the effect and the increased numerical uncertainty at large R_0 values it is, however, hard to judge whether or not it is a real effect.

B. Local density of states

An understanding of the reduced H_2 binding in metals can be obtained by looking at the local induced density of states for H_2 ($R_0 = 1.4$ a.u.) at different r_s values. In Fig. 5 I show for simplicity only the Σ ($m = 0$) part of ΔD^L. In vacuum, the usual picture appears: The two 1s hydrogen states interact to give an even (Σ_g) bonding and an odd (Σ_u) antibonding state. Because the latter lies

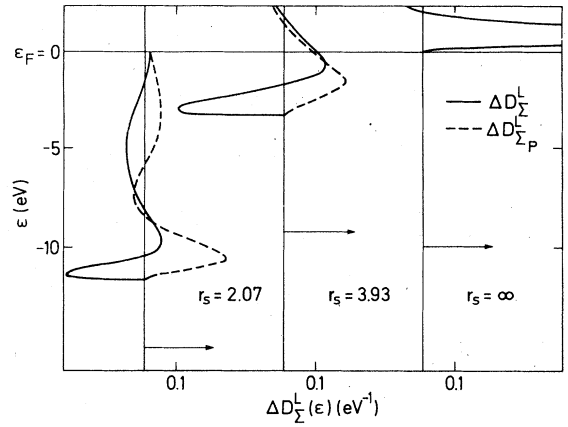

FIG. 5. The Σ and Σ_p parts (see text) of the local induced density of states for free H_2 and H_2 in jellium for $r_s = 2.07$ and 3.93, corresponding to Al and Na, respectively.

above the vacuum level, it shows up as a resonance. The strong binding in free H_2 is then a consequence of the fact that only the bonding state is filled. For the other r_s values in Fig. 5, ΔD_Σ^L is more complex. A bonding-type (even) bound state is retained, but the mixing of even and odd states blurs out the structure above the bottom of the band. ΔD_Σ^L has been resolved into its partial-wave components. In Fig. 5 the p part is represented by dashed curves. It shows for all r_s values a pronounced resonance structure just above the bottom of the band. Since these p states are odd, the p resonance can be regarded as part of the antibonding H_2 resonance. It is seen that the decrease in binding energy is completely correlated with the filling of the antibonding resonance. At Al density, where it is completely filled, the interaction resembles the He-He interaction.

On this basis the hydrogen impurity-impurity interaction in free-electron-like metals can be described in the following way: As two hydrogen impurities approach each other, the two shallow H^--like bound states (see Fig. 2) split up into a bonding and an antibonding state (resonance). Since the position of the antibonding resonance relative to the bottom of the band is approximately independent of r_s, the resonance gets filled except for the very lowest densities (smallest Fermi energies), and the interaction becomes repulsive. The extra electrons connected with the antibonding resonance are screened out by primarily spherically symmetrical distorted plane-wave states near the bottom of the band. This is similar to the single-impurity case where the extra bound electron was also screened out by an antiresonance in the bottom of the band (see Fig. 2). The antiresonance in the s part of ΔD_Σ^L can be regarded as a reminiscence of that in Fig. 2, broadened because of interactions.

VI. SUMMARY

The description of the electron structure of hydrogen impurities in metals as described by the jellium model is completed with a presentation of the hydrogen-induced density of states. These spectra have two functions.

First, they can provide a basis for an understanding of the electron structure of the impurity in question. For single hydrogen the apparent conflict between the existence of a very shallow H^--like bound state and an induced density, which is even more contracted than that of free hydrogen, is resolved by realizing that the electron is screened out primarily by the long-wavelength conduction electrons in the bottom of the band. The repulsive H-H interaction found in most metals is also understandable from the H_2-induced density of states: the antibonding H_2 molecular orbital is filled at normal metallic densities.

Second, the spectra for single impurities are shown to represent the true excitation spectra quite well. This is done by comparing the one-electron bound-state energy parameter with spin-polarized ΔSCF calculations and with the many-body calculations of Vinter.[28] The fact that the hydrogen-induced structure is shown to follow closely the local bottom of the band, so that the bound state found for hydrogen in bulk jellium is turned into a resonance in the middle of the conduction band for hydrogen in a vacancy, suggests that interstitial and substitutional hydrogen in free-electron-like metals can be distinguished experimentally by their excitation spectra.

ACKNOWLEDGMENTS

The author is grateful to H. Hjelmberg and B. I. Lundqvist for many discussions and suggestions and to the latter for critically reading the manuscript.

[1]W. Eichenauer, Z. Metallkd. 59, 613 (1968).
[2]J. Völkl and G. Alefeld, in *Diffusion in Solids*, edited by A. S. Norwick and J. J. Burton (Academic, New York, 1975).
[3]For interactions with vacancies see, e.g., D. Lengeler, S. Mantl, and W. Triftshäuser, J. Phys. F 8, 1691 (1978). For mutual interactions see, e.g., J. Bøttiger, S. T. Picraux, N. Rud, and T. Laursen, J. Appl. Phys. 48, 920 (1977).
[4]J. P. van Dyke, Nucl. Mater. 69 & 70, 533 (1978); R. W. Simpson, N. F. Lane, and R. C. Cloney, Nucl. Mater. 69 & 70, 582 (1978).
[5]W. Kohn and L. J. Sham, Phys. Rev. 140, A1133 (1965).
[6]Z. D. Popovic and M. J. Stott, Phys. Rev. Lett. 33, 1164 (1974).
[7]C. O. Almbladh, U. von Barth, Z. D. Popovic, and M. J. Stott, Phys. Rev. B 14, 2250 (1976).
[8]E. Zaremba, L. M. Sander, H. B. Shore, and J. H. Rose, J. Phys. F 7, 1763 (1977).
[9]P. Jena and K. S. Singwi, Phys. Rev. B 17, 3518 (1978).
[10]M. Manninen, P. Hautojärvi, and R. Nieminen, Solid State Commun. 23, 795 (1977).
[11]J. K. Nørskov, Solid State Commun. 24, 691 (1977).
[12]M. D. Whitmore, J. Phys. F 6, 1259 (1976).
[13]M. D. Whitmore, Phys. Lett. A 55, 57 (1975).
[14]G. W. Bryant (unpublished).
[15]J. K. Nørskov, Solid State Commun. 25, 995 (1978).
[16]O. Gunnarsson and H. Hjelmberg, Phys. Scr. 11, 97 (1975).
[17]H. Hjelmberg, Phys. Scr. 18, 481 (1978).
[18]Z. D. Popovic, M. J. Stott, J. P. Carbotte, and G. R. Piercy, Phys. Rev. B 13, 590 (1976).

[19]H. Hohenberg and W. Kohn, Phys. Rev. 136, B864 (1964).
[20]O. Gunnarsson and B. I. Lundqvist, Phys. Rev. 13, 4274 (1976).
[21]See, e.g., C. P. Flynn, *Point Defects and Diffusion* (Clarendon, Oxford, 1972), p. 725.
[22]For $r_s \gtrsim 5$, ϵ_b starts to decrease. This may, however, be connected with the problems encountered in the local-density approximation for the H^- ion. See O. Gunnarsson, M. Jonson, and B. I. Lundqvist, Phys. Rev. B (to be published) and Ref. 8 for a discussion of this point.
[23]J. E. Inglesfield and J. B. Pendry, Philos. Mag. 34, 205 (1976).
[24]See, e.g., N. F. Mott and H. S. W. Massey, *The Theory of Atomic Collisions* (Clarendon, Oxford, 1965), p. 43.
[25]See, e.g., Ref. 21, p. 732.
[26]H. Hjelmberg, O. Gunnarsson, and B. I. Lundqvist, Surf. Sci. 68, 158 (1977).
[27]N. D. Lang and A. R. Williams, Phys. Rev. B 18, 616 (1978).
[28]B. Vinter, Phys. Rev. B 17, 2429 (1978).
[29]The results of Fig. 4 are somewhat different from those of Ref. 15 due to a numerical error in the latter results.